METHODOLOGY Open Access



Assessing and avoiding C isotopic contamination artefacts in mesocosm-scale $^{13}\text{CO}_2/^{12}\text{CO}_2$ labelling systems: from biomass components to purified carbohydrates and dark respiration

Jianjun Zhu^{1,2}, Regina T. Hirl¹, Juan C. Baca Cabrera^{1,3}, Rudi Schäufele^{1,4*} and Hans Schnyder^{1*}

Abstract

Background Quantitative understanding of plant carbon (C) metabolism by $^{13}\text{CO}_2/^{12}\text{CO}_2$ -labelling studies requires absence (or knowledge) of C-isotopic contamination artefacts during tracer application and sample processing. Surprisingly, this concern has not been addressed systematically and comprehensively yet is especially crucial in experiments at different atmospheric CO₂ concentrations ([CO₂]), when experimental protocols require frequent access to the labelling chambers. Here, we used a plant growth chamber-based $^{13}\text{CO}_2/^{12}\text{CO}_2$ gas exchange-facility to address this topic. The facility comprised four independent units, with two chambers routinely operated in parallel under identical conditions except for the isotopic composition of CO₂ supplied to them ($\delta^{13}\text{C}_{\text{CO2}}$ –43.5% *versus* –5.6%). In this setup, $d\delta^{13}\text{C}_{\chi}$ (the measurements-based $\delta^{13}\text{C}$ -difference between matching samples *X* collected from the parallel chambers) is expected to equal $d\delta^{13}\text{C}_{\text{Ref}}$ (the predictable, non-contaminated $\delta^{13}\text{C}$ -difference), if sample-C is completely derived from the contrasting CO₂ sources. Accordingly, contamination (f_{contam}) was determined as f_{contam} = 1– $d\delta^{13}\text{C}_{\chi}/d\delta^{13}\text{C}_{\text{Ref}}$ in this experimental setup. Determinations were made for biomass fractions, water-soluble carbohydrate (WSC) components and dark respiration of *Lolium perenne* (perennial ryegrass) stands following growth for ~9 weeks at 200, 400 or 800 μmol mol⁻¹ CO₂, with a terminal two weeks-long period of extensive experimental disturbance of the chambers.

Results Contamination was small and similar (average $3.3\% \pm 0.9\%$ SD, n = 18) for shoot and root biomass and WSC fractions (fructan, sucrose, glucose, fructose) at every $[CO_2]$ level. $[CO_2]$ had no significant effect on contamination of these samples. There was no evidence for any contamination of WSC components during extraction, separation and analysis. At 200 and 400 μ mol mol⁻¹ CO₂, contamination of respiratory CO₂ was close to that of biomass- and WSC-C, suggesting it originated primarily from in vivo-contaminated respiratory substrate. Surprisingly, we found no evidence

*Correspondence: Rudi Schäufele schaeufele@tum.de Hans Schnyder schnyder@tum.de

Full list of author information is available at the end of the article



© The Author(s) 2025. **Open Access** This article is licensed under a Creative Commons Attribution 4.0 International License, which permits use, sharing, adaptation, distribution and reproduction in any medium or format, as long as you give appropriate credit to the original author(s) and the source, provide a link to the Creative Commons licence, and indicate if changes were made. The images or other third party material in this article are included in the article's Creative Commons licence, unless indicated otherwise in a credit line to the material. If material is not included in the article's Creative Commons licence and your intended use is not permitted by statutory regulation or exceeds the permitted use, you will need to obtain permission directly from the copyright holder. To view a copy of this licence, visit http://creativecommons.org/licenses/by/4.0/.

Zhu et al. Plant Methods (2025) 21:111 Page 2 of 17

of contamination of respiratory CO_2 at 800 μ mol mol⁻¹ CO_2 . Overall, contamination likely resulted overwhelmingly from photosynthetic fixation of extraneous contaminating CO_2 which entered chambers primarily during daytime experimental activities.

Conclusions The labelling facility enables months-long, quantitative $^{13}CO_2/^{12}CO_2$ -labelling of large numbers of plants with accuracy and precision across contrasts of $[CO_2]$, empowering eco-physiological study of climate change scenarios. Effective protocols for contamination avoidance are discussed.

Keywords Atmospheric CO_2 concentration, Bulk carbon, ^{13}C isotopic labelling, ^{13}C discrimination, Isotopic fractionation, C tracer, CO_2 gas exchange, Contamination, Experimental artifact, Water-soluble carbohydrates (fructan, sucrose, glucose, fructose)

Background

Isotopic labelling of the carbon (C) in CO₂ supplied to photosynthesizing organisms is a unique and powerful method for investigating C fluxes in central metabolism, transport, allocation and partitioning of photosynthetic products from the organelle (chloroplast) to the ecosystem scale [1-17]. Multiple different techniques, including pulse-chase and dynamic labelling (sensu Ratcliffe & Shachar-Hill [18]; or synonymous 'steady-state' or 'continuous' labelling [7]) with different C isotopes (11C, 13C or 14C) have been designed and applied to different aspects of the analysis of C fluxes in plants [6, 7, 19-22]. One such method is especially useful for longterm (hours- to months-long) labelling at large scales, with large numbers of plants in controlled environments, and uses inexpensive and harmless near-natural abundance ¹³CO₂/¹²CO₂ mixtures [21, 23–25]. These are derived from ¹³C-depleted fossil-organic or (relatively) ¹³C-enriched mineral sources and thus termed 'fossilorganic' or 'mineral CO2'. This technique has proven useful for the determination of functional components of CO₂ fluxes, such as dark respiration in light [25, 26], distinction of autotrophic and heterotrophic ecosystem respiration [21] and quantification of the labelling kinetics of metabolic and storage substrate pools supplying sink tissue [27, 28] or dark respiration of shoots and roots [29, 30]. Further, such tracer studies have enabled analysis of C fluxes in central carbohydrate metabolism of source leaves and of the function and importance of assimilate stores (or reserves) in supplying substrate to growth or respiration by compartmental models at organ, plant and ecosystem scale [27, 31–33].

A special variant of this labelling strategy– particularly useful for systematic and comprehensive exploration of common contamination artefacts (as we show here)– uses two parallel identical growth chambers with the same plant material grown in the same conditions except for the C isotopic composition ($\delta^{13} \text{C}$, Table 1) of the CO $_2$ ($\delta^{13} \text{C}_{\text{CO2}}$) supplied to the chambers. In our laboratory, such a system is directly connected with a continuous-flow stable isotope ratio mass spectrometer (CF-IRMS) which permits quasi-continuous monitoring of $\delta^{13} \text{C}_{\text{CO2}}$

at the chamber inlet and outlet of the air stream passing through the chambers (Fig. 1). As air is ventilated strongly inside the chambers, the $\delta^{13}C_{CO2}$ at the chamber outlet reflects that inside the chamber [25] as in leaf cuvettes [34].

In the field, as well as in open experimental systems (such as flow-through leaf cuvettes or mesocosms, as here), the δ^{13} C of plant biomass is generally 13 C-depleted relative to CO_2 because of 13 C discrimination (Δ^{13} C), i.e. isotopic fractionation against 13 C, in photosynthesis [35, 36], possibly modified further to a smaller degree by post-photosynthetic isotopic fractionation effects [29, 37–40]. According to Farquhar et al. [35, 36], δ^{13} C of a given plant sample X (tissue or compound) is related to $\delta^{13}C_{CO2}$ as.

$$\delta^{13}C_X = (\delta^{13}C_{CO2} - \Delta^{13}C_X)/(1 + \Delta^{13}C_X), (1)$$

with $\Delta^{13}C_X$ representing the sample-specific $\Delta^{13}C$ (which integrates both photosynthetic and eventual post-photosynthetic effects). Although $\Delta^{13}C_X$ can vary as a function of environmental conditions [41, 42], it is theoretically independent of the isotopic composition of CO_2 [36] and, hence, must be the same when plants are grown in identical conditions with different $\delta^{13}C_{CO2}$ [24, 25].

Therefore, when established in the above two-chamber system, the δ^{13} C of an uncontaminated (pure) plant C sample (termed $\delta^{13}C_{Ref}$) which is synthesized completely from photosynthetic CO₂ uptake of a certain CO₂ source is expected to accord with Eq. 1 independently of the $\delta^{13}C_{CO2}$ of the source CO₂. Accordingly– and again in artefact-free conditions and steady-state– the δ^{13} Cdifference $(d\delta^{13}C_{Ref})$ between chambers supplied with ¹³C-enriched (mineral) and ¹³C-depleted (fossil) CO₂ should be identical to that predicted using Eq. 1. Any C contamination of an actual sample X would cause a (contamination-weighted) decrease of $d\delta^{13}C_{X \ actual}$ relative to $d\delta^{13}C_{Ref}$ (i.e. $d\delta^{13}C_{X \text{ actual}} < d\delta^{13}C_{Ref}$). In the extreme, where $d\delta^{13}C_X = 0$, the sample X is fully independent of the different $\delta^{13}C_{\text{CO2}}$ used, i.e. is completely contaminated. Accordingly, the fraction of contaminating C in a certain sample $X(f_{\text{contam }X})$ can be defined as:

Zhu et al. Plant Methods (2025) 21:111 Page 3 of 17

 Table 1
 Definition of symbols, and specifications

Symbol	Definition	Specification	
δ ¹³ C	Defined as $\delta^{13}C = (R_p/R_s-1) \times 1000$, with R the molar abundance ratio $^{13}C/^{12}C$, and P referring to the sample and S to the international Vienna-Pee Dee Belemnite (V-PDB) standard (‰)	Farquhar et al. [36]	
δ ¹³ C _{CO2}	δ ¹³ C of CO ₂ (‰)	Here we used CO $_2$ of mineral ($\delta^{13}C_{CO2}$ ~-5.6%) and fossil-organic origin ($\delta^{13}C_{CO2}$ ~-43.5%) to supply parallel growth chambers	
$\delta^{13}C_{inlet}$	δ^{13} C of CO ₂ at the inlet of a growth chamber (‰)	Measured	
$5^{13}C_{outlet}$	δ^{13} C of CO ₂ at the outlet of a growth chamber (‰)	Measured	
$\delta^{13}C_{ m outlet}$ pure	$\delta^{13} \text{C}$ of uncontaminated CO_2 at the outlet of a growth chamber (‰)	Calculated as: $\delta^{13}C_{outlet pure} = (\Delta^{13}C + \xi \delta^{13}C_{inlet} \Delta^{13}C/1000 + \xi \delta^{13}C_{inlet})/($ $\Delta^{13}C/1000 (\xi - 1) + \xi),$ with $\Delta^{13}C$ fixed at 21%	
δ ¹³ C _X	δ^{13} C of sample X (‰), with X referring to net photosynthesis, dark respiration, biomass, or WSC in the form of fructan, sucrose, glucose or fructose	Measured	
$\delta^{13}C_{WSC}$	δ^{13} C of water-soluble carbohydrates (WSC) (‰)	Measured	
$\delta^{13}C_{WSC-free}$ biomass	δ^{13} C of WSC-free biomass (‰)	Calculated as $\delta^{13} C_{WSC-free\;biomass} = (\delta^{13} C_{biomass} \times W_{biomass} - \delta^{13} C_{WSC} \times W_{WSC}) / (W_{biomass} - W_{WSC})$	
dδ ¹³ C _X	δ^{13} C-difference between samples of the same kind (net photosynthesis, dark respiration, biomass, or WSC, in the form of fructan, sucrose, glucose or fructose) collected simultaneously from parallel chambers supplied with CO ₂ of contrasting δ^{13} C _{CO2} (‰)	Based on measurements	
$\delta^{13}C_{Ref}$	$\delta^{13}\text{C}$ of uncontaminated (pure) reference (‰)	Calculated as $\delta^{13} C_{\text{Ref}} = (\delta^{13} C_{\text{inlet}} \times F_{\text{inlet}}^{-} - \delta^{13} C_{\text{outlet pure}} \times F_{\text{outlet}}) / (F_{\text{inlet}}^{-} - F_{\text{outlet}})$	
$d\delta^{13}C_{Ref}$	$\delta^{13}\text{C-difference}$ between uncontaminated (pure) references from parallel chambers supplied with CO $_2$ of contrasting $\delta^{13}\text{C}_{\text{CO2}}$ (%))	Based on calculations of $\delta^{13} C_{Ref}$ for 'samples' collected simultaneously from parallel chambers supplied with contrasting $\delta^{13} C_{CO2}$	
f _{contam X}	Fraction of contaminating C in sample X	Calculated as $1 - d\delta^{13}C_X/d\delta^{13}C_{Ref}$	
Δ^{13} C	Carbon isotope discrimination (‰)	Farquhar et al. [36], here set to 21‰ in estimations of $\delta^{13}C_{Ref}$	
$\Delta^{13}C_X$	Carbon isotope discrimination as expressed in sample X (‰)	Based on measurements, and calculated as $\Delta^{13}C_X = (\delta^{13}C_{outlet} - \delta^{13}C_X)/(1 + \delta^{13}C_X/1000)$	
ξ	Ratio of the rate of ${\rm CO_2}$ entry into a growth chamber relative to the net rate of ${\rm CO_2}$ uptake (net photosynthesis)	After Evans et al. [34] Calculated as $\xi = C_{inlet} / (C_{inlet} - C_{outlet})$	
[CO ₂]	CO_2 concentration in air (µmol mol ⁻¹)		
C _{inlet}	${\rm CO_2}$ concentration in air at the inlet of the growth chamber ($\mu {\rm mol \ mol^{-1}}$)	Measured	
C _{outlet}	${\rm CO_2}$ concentration in air at the outlet of the growth chamber ($\mu {\rm mol \ mol^{-1}}$)	Measured	
Finlet	Flux of CO_2 entering a growth chamber (μ mol s ⁻¹)	Based on measurements	
Foutlet	Flux of CO_2 leaving a growth chamber (μ mol s ⁻¹)	Based on measurements	
Α	Ground area of a growth chamber (m²)		
N	Net CO_2 exchange rate in light, i.e. whole-stand net photosynthesis rate (μ mol m $^{-2}$ s $^{-1}$)	$N = (F_{\text{inlet}} - F_{\text{outlet}}) / A$, during daytime	
R _n	Whole-stand respiration rate in the dark (μ mol m $^{-2}$ s $^{-1}$)	$R_{\rm n} = (F_{\rm inlet} - F_{\rm outlet}) / A$, during nighttime	
$W_{ m biomass}$	C mass of a certain biomass sample (g)	Measured	
W _{WSC}	C mass of WSC in a certain sample (g)	Based on measurements and the mass fraction of C in different forms of water-soluble carbohydrates (fructan ~ 0.44, sucrose 0.42, glucose and fructose 0.40)	
X	Designation of samples of a given kind collected simultaneously from parallel chambers supplied with contrasting CO ₂ ; may refer to dark respiration, biomass, or WSC (fructan, sucrose, glucose, fructose)	Here, CO_2 of mineral ($\delta^{13}C_{CO2} \sim -5.6\%$) or fossil-organic ($\delta^{13}C_{CO2} \sim -43.5\%$) origin	

Zhu et al. Plant Methods (2025) 21:111 Page 4 of 17

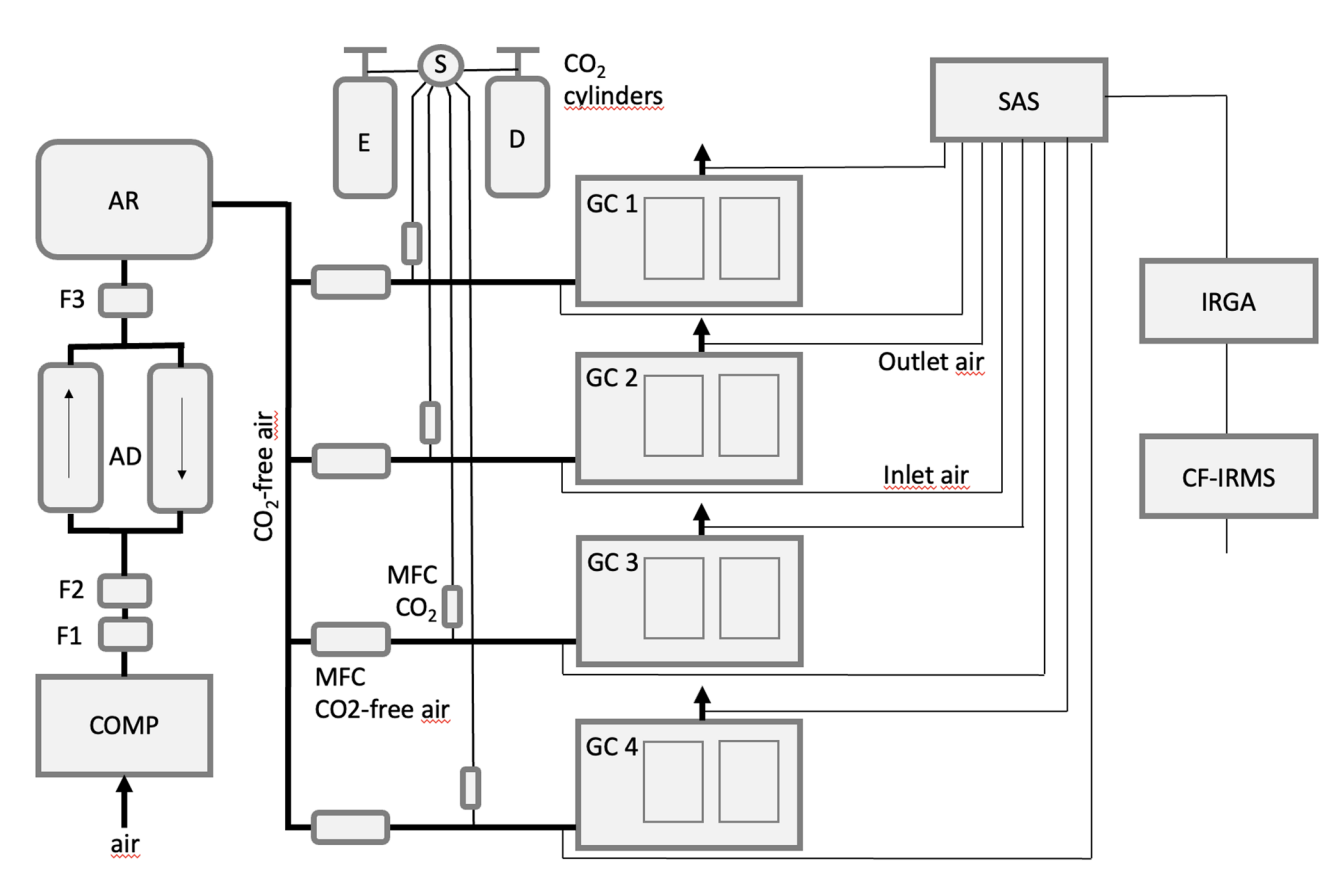


Fig. 1 Schematic diagram of the ¹³CO₂/¹²CO₂ labelling and gas exchange system. COMP, screw compressor (S40, Boge, Bielefeld, Germany); F1, oil and water condensate drain (CSP005; Hiross, Mönchengladbach, Germany); F2, oil, water and particle filter (≥ 0.01 μm; G12XD, with filter element 2030X, Zander); AD, adsorption dryer (KEN 3100 TE; Zander, Essen, Germany) and molecular sieve: activated aluminium oxide F200; Alcoa, Houston, TX, USA); F3, universal filter (≥ 1 μm; G12ZHD and filter element: 2030Z, Zander); AR, air receiver (1 m³) (Magnet Kft, Magocs, Hungary); E and D, cylinders with ¹³C-depleted (fossil) and -enriched (mineral) CO₂ from Linde AG (Unterschleissheim, Germany) and CARBO Kohlensäurewerke (Bad Hönningen, Germany); S, CO₂ source unit for mineral and fossil-organic CO₂ (DMP Ltd, Fehraltdorf, Switzerland); MFC CO₂, CO₂ mass flow controller (Red-y, Vögtlin, Muttenz, Switzerland, max 1 SLPM); MFC air, mass flow controller for CO₂ free air (EL-FLOW, Bronkhorst, Veenendaal, Netherlands; 1000 SLPM); GC 1–4, growth chambers (PGR15; Conviron, Winnipeg, Canada); SAS, sample air selector (DMP Ltd, Fehraltdorf, Switzerland); IRGA, CO₂ and H₂O infrared gas analyser (Li-840, Li-Cor Inc., Lincoln, NE, USA); CF-IRMS, continuous-flow ¹³CO₂/¹²CO₂ isotope ratio mass spectrometer (Delta plus; Finnigan MAT, Bremen, Germany). For simplicity, a number of auxillary components of the facility are not included in the figure (but see text)

$$f_{\text{contam X}} = 1 - d\delta^{13} C_{\text{X actual}} / d\delta^{13} C_{\text{Ref}}.$$
 (2)

Ceteris paribus, a given contaminating C source has the same δ^{13} C and adds the same quantity of C to a certain sample X collected from the parallel chambers which are fed with different $\delta^{13}C_{CO2}$. This is true especially, if the parallel chambers are operated simultaneously, are housed in the same room, and sample collection and processing use identical protocols (as was the case in this work). Putative contaminating C sources are many and include (1) free atmospheric CO_2 (which has a $\delta^{13}C$ of approx. -9% at present [43]), (2) CO₂ exhaled by people (e.g. experimenters; -17 and -25% [44, 45]), and (3) cross-contamination with the different labelling CO₂s [24, 25]. Further, (4) contamination with organic C compounds might occur during sample collection or processing [46, 47]. In the context, also (5) seed biomass-C (or biomass of any type of experimental starting material, e.g. vegetative cuttings or seedlings) 'qualifies' as a contaminant, as it shares the same $\delta^{13}C$ in the different labelling chambers. Particularly, in climate change experiments, the likelihood and extent of contamination could perhaps depend on the atmospheric CO_2 concentration, $[CO_2]$, which is used in the experiments. This would cause a $[CO_2]$ -dependent experimental artefact and bias conclusions, if unnoted or uncorrected. As far as we know, there have been no systematic, comprehensive analyses of contamination artefacts in large- or stand-scale, long-term C labelling studies (but see Gong et al. [26]). Particularly, we know of no such methodological study under sub-ambient or elevated $[CO_2]$ conditions.

In this work, we ask: How does $[CO_2]$ affect C contamination $(f_{\rm contam})$ of a range of parameters that are of interest in labelling studies, including biomass fractions (shoot and root), non-structural carbohydrate components (water-soluble carbohydrates (WSC): fructan, sucrose, glucose, fructose) and dark respiration? In

Zhu et al. Plant Methods (2025) 21:111 Page 5 of 17

addition, we perform a sensitivity analysis of C isotope discrimination (Δ^{13} C) assumptions on the estimates of contamination. At the outset, we provide a description of the custom-made labelling facility used here. The work was performed with stands of Lolium perenne (perennial ryegrass, C₂) established from 12 days-old seedlings grown in parallel growth chambers under identical conditions with contrasting $\delta^{13}C_{CO2}$ (i.e. $\delta^{13}C_{CO2}$ of –43.5% or -5.6‰) at 200, 400 or 800 μmol mol⁻¹ CO₂, approximating Last Glacial Maximum, current ambient, or predicted end-of-the 21st century [CO₂] levels [48]. Biomass samples for contamination analysis were collected immediately after the terminal, two weeks-long experimental period in which the labelling vessels (growth chambers) had to be accessed frequently for plant sampling or nondestructive measurements [48–50]. These perturbations provided a special opportunity for contamination of the chamber atmospheres with extraneous CO₂.

Materials and methods

Mesocosm-scale $^{13}\mathrm{CO}_2/^{12}\mathrm{CO}_2$ gas exchange and labelling system

The $^{13}\text{CO}_2/^{12}\text{CO}_2$ gas exchange and labelling facility corresponded to a modernized and upgraded version of the system originally described by Schnyder et al. [25]. The facility was composed of four main modules (Figs. 1, S1 and S2): (1) a screw compressor and adsorption dryer which generated CO₂-free air, (2) a gas mixing system which controlled the addition of CO₂ to CO₂-free air and supplied air with known $\delta^{13}\text{C}_{\text{CO2}}$ and [CO₂] at an individually set rate for both air flow and [CO₂] to each labelling vessel, (3) four plant growth chambers, which served as the labelling vessels, and (4) a gas analysis unit, comprising a sample air selector, an infrared CO₂ gas analyzer (IRGA) and a continuous flow $^{13}\text{CO}_2/^{12}\text{CO}_2$ IRMS, which analyzed in sequence the [CO₂] and $\delta^{13}\text{C}_{\text{CO2}}$ of sample gas collected at the inlet and outlet of each chamber.

Specifically, the four growth chambers served as opensystem [51], mesocosm-scale gas exchange cuvettes, each having a 1.5 m² plant growth area and equipped with a microprocessor controller and environmental data acquisition system. All air supply to a growth chamber was provided by a dedicated gas mixing station which consisted of two computer-controlled mass flow controllers (Fig. 1) which regulated the mixing of CO₂ with known δ^{13} C (0–1 standard liter per minute, SLPM) and CO₂-free air (0-1000 SLPM). Dry CO₂-free air was obtained with a self-regenerating adsorption dryer at up to 180 m³ h⁻¹ at ambient atmospheric pressure. The dryer was fed with compressed air (approx. 7 MPa) by a screw compressor via an oil and water condensate drain and filters as shown in Fig. 1. Commercially available CO₂ of known δ^{13} C was supplied from cylinders (Fig. 1). Typically, rates of air supply to individual chambers ranged between 250 and 750 SLPM. Thus, with an internal chamber volume of approx. 3000 L, air flow through a chamber was equal to 5-15 times the chamber volume per hour. Accordingly, the mean residence time of CO₂ in the chamber was 4-12 min. Sample air was collected at the inlet and outlet of each growth chamber and continuously pumped to the computer-controlled sample air selector (SAS) at a rate of approx. 2 L min⁻¹. During simultaneous operation of all chambers the SAS sequentially sampled each sample air line (n = 8; Fig. 1) at approx. 3 minutes-intervals. Sample air was split to serve the IRGA and CF-IRMS in parallel. Gas lines between the SAS and CF-IRMS and IRGA were flushed with sample air for 3 min before taking IRGA readings of CO2 and H2O concentration and measurement of δ^{13} C by the CF-IRMS. The CF-IRMS was interfaced with the sample air selector via a steel capillary tube (1 mm i.d.), a eight-port, two-position valve (Valco Instruments Co. Inc., Houston, TX, USA), dryer (Nafion[®]), gas chromatograph (25 m × 0.32 mm Poraplot Q; Chrompack, Middelburg, Netherlands) and open split. These components all formed part of a custom-made interface (Gasbench II; ThermoFinnigan, Bremen, Germany). Sample air for the CF-IRMS was pumped continuously through the steel capillary feeding the Valco valve and a 0.25 mL sample loop attached to it. After a 90 s flushing period, the content of the sample loop was swept with helium carrier gas through the interface, where water vapor was removed by the Nafion trap and CO₂ was separated from other sample air gases in a GC column. Finally, the CO₂ was introduced directly into the ion source of the IRMS via a glass capillary (0.1 mm i.d.) connected to the interface by an open split. After another 90 s, shortly before the sample air selector switched to the next sample air line, a second sample of the same air was taken. Thus, within 3 min, each inlet/ outlet was measured in duplicate. After every second sample, a VPDB-gauged CO2 reference gas was injected into the CF-IRMS via the open split. A full measurement cycle, including one set of measurements (concentrations of CO₂ and H₂O, and δ^{13} C of CO₂) on the inlet and outlet of each growth chamber, was completed within less than 30 min. The long-term precision (SD) for repeated measurements at the chamber inlet was < 0.20%.

Empty chamber tests performed before every experiment confirmed that gas lines throughout the air supply systems of the chambers were virtually leak-free based on measurements with $\rm CO_2$ free air generated by the adsorption dryer and CF-IRMS based measurement of the peak size (observed peak area corresponded to a $\rm CO_2$ concentration of $<<0.5~\mu\rm mol~mol^{-1})$ of mass 44, i.e. $^{12}\rm C^{16}\rm O_2$, at the chamber inlet. The same was true for measurements at the chamber outlet, when the flow rate of $\rm CO_2$ -free air was maintained at $>250~\rm SLPM$, as was routinely the case in experiments.

Zhu et al. Plant Methods (2025) 21:111 Page 6 of 17

Individual CO_2 cylinders contained approx. 30 kg of CO_2 , and more than one cylinder had to be used in experiments of long duration (>4 weeks). For this reason, we examined batches of CO_2 cylinders for uniformity of their $\delta^{13}C_{CO2}$. Typically, the $\delta^{13}C_{CO2}$ was quite similar (<0.27% SD) between cylinders of the same type (mineral or fossil-organic CO_2) within a batch.

Plant material and growth conditions

The details for the plant material and growth conditions used in this study have been presented before [48-50]. In short, plants of Lolium perenne were established and grown singly in individual plastic pots (350 mm height, 50 mm diameter) filled with 800 g of washed quartz sand (0.3-0.8 mm grain size). Pots were arranged at a density of 383 plants m⁻² in plastic containers (770×560×300 mm), and two of such containers placed in each growth chamber. Plants were supplied four times a day with a Hoagland-type nutrient solution with reduced nitrate-N content [48]. Light was supplied by cool-white, fluorescent tubes and warm-white, lightemitting diode (LED) bulbs with a constant photosynthetic photon flux density (PPFD) of 800 µmol m⁻² s⁻¹ at plant height during the 16 h-long light period [48]. Temperature was controlled at 20 °C/16°C and relative humidity (RH) at 50%/75% during the light/dark periods. Importantly, we observed no chamber effects on any measured parameter in the studies of Baca Cabrera et al. [48-50].

$[CO_2]$ treatments and sequence of experimental activities and sampling

 $[CO_2]$ treatments were installed when seedlings were 12 days old following seed imbibition. In each of two experimental runs chamber air was controlled near the target CO_2 concentration ($[CO_2]$ of 200, 400 or 800 μmol $^{-1}$) [48] with two chambers per $[CO_2]$ treatment. In that, one chamber was supplied with ^{13}C -enriched (mineral) CO_2 and the other with ^{13}C -depleted (fossil-organic) CO_2 . Maintenance of $[CO_2]$ near target values throughout the experiment– from 12 days-old seedlings to closed stands and beyond– required periodic adjustments of airflow and $[CO_2]$ at the chamber inlet. This was done in such a way that the (photosynthetic) drawdown of $[CO_2]$ inside the chambers did not exceed 14%. Quasi-continuous $^{13}CO_2/^{12}CO_2$ measurements at the inlet and outlet of chambers were performed from day 20 to at least day 65.

Disturbance of the $[CO_2]$ and $\delta^{13}C_{CO2}$ in the chambers was minimized by maintaining a small overpressure in the chambers relative to the outside atmosphere (Figure S2D) and by restricting daytime experimental activities inside the chambers between days 49 and 63 as much as possible within the limitations of the experimental plan [48–50]. Also, air locks (Figure S3A) were installed in

chamber doors throughout the 14 days-long period of active experimentation. For the latter chambers had to be routinely accessed daily before the end of the light period for (non-destructive) measurements of leaf elongation on eight plants per chamber [48]. In parallel, leaf level gas exchange measurements (not reported here) were made on individual plants [48]. These measurements were performed in a different, dedicated growth chamber which was controlled at the same [CO₂] with the same δ^{13} C_{CO2} as the chamber of origin of a given plant. Thus, individual plants were removed from their chambers for leaf level gas exchange measurements and later returned to their chamber of origin [48]. In addition, intensive sampling activities over two consecutive days occurred before the end of the light and dark periods on days 49 and 50, and days 63 and 64 (data not reported here, but partly presently in Baca Cabrera et al. [49, 50]).

The above activities intrinsically meant a disturbance which generated opportunities for contamination of the chamber atmospheres with extraneous CO₂ (Fig. 2). Here, we quantify the cumulative effect of all putative sources of contamination (see Background) on the δ^{13} C of plant biomass and WSC components. For this, we sampled plants shortly after the end of the intensive experimental period (day 65) at the beginning of the dark period. Two replicate samples from each growth chamber were collected, with one replicate consisting of three randomly selected plants. Plants were removed from their pot, their roots washed to free them of sand and dissected into their shoot and root parts. The plant parts were weighed to determine their fresh weight, then frozen in liquid nitrogen and stored at -18 °C before freeze-drying for 72 h. Dry weights were subsequently determined. After that, plant material was ground to a fine powder in a ball mill (Mixer mill MM 400, Retsch, Haan, Germany) in 2-mL stainless steel grinding jars with 0.5-mm stainless steel beads, and thereafter stored again at -18 °C until further use.

WSC extraction and separation

WSC were extracted from shoot samples and fractions (fructan, sucrose, glucose, and fructose) separated using the procedures described by Gebbing & Schnyder [52]. Briefly, aliquots of 200 mg of milled sample material were weighed into 2-mL capped Eppendorf tubes and topped off with 1.8 mL of deionized water. Tubes were briefly vortexed (Vortex-Genie 2, Scientific Industries, New York, USA), held in a water bath at 93 °C for 10 min, shaken for 45 min (Shaker, Heidolph Instruments, Schwabach, Germany) at room temperature, and then centrifuged at 9500 g for 15 min (Universal 320, Merck, Tuttlingen, Germany). The supernatant, which contained the dissolved WSC, was passed through nylon-membrane

Zhu et al. Plant Methods (2025) 21:111 Page 7 of 17

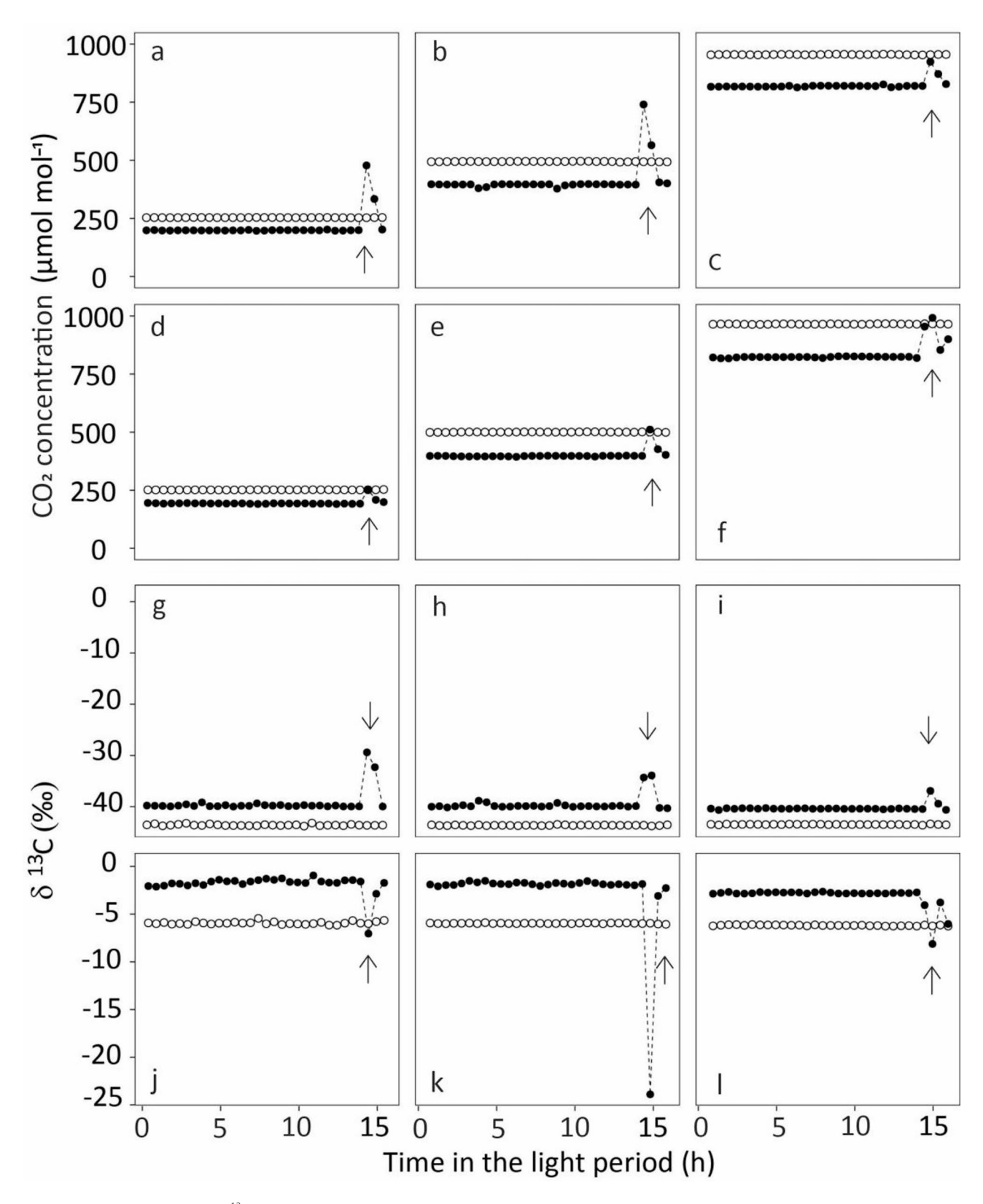


Fig. 2 Concentration (a - f) and δ^{13} C (g - l) of CO₂ inside growth chambers during one light period. Growth chambers were maintained near target [CO₂] of 200 (a, d, g and j), 400 (b, e, h and k), or 800 (c, f, i and l) μ mol mol⁻¹ with either ¹³C-depleted CO₂ (δ^{13} C_{CO2} -43.5‰) (a, b, c, g, h, and i) or ¹³C-enriched CO₂ (δ^{13} C_{CO2} -5.6‰; right) (d, e, f, j, k, and l). Open circles denote measurements at the chamber outlet, and closed circles at the chamber inlet. Vertical arrows indicate chamber door openings during sampling activities on day 49. Data points represent individual measurements

Zhu et al. Plant Methods (2025) 21:111 Page 8 of 17

filters with a pore size of 0.45 μm and then stored in clean 2-mL capped Eppendorf tubes at -18 °C.

WSC fractions (fructan, sucrose, glucose and fructose) were separated, quantified and collected using a highperformance liquid chromatography (HPLC) system similar to that of Gebbing & Schnyder [52]. Thus, 0.2 mL aliquots of the filtered supernatant were passed through a guard column (Shodex KS-LG, Showa Denko, Tokyo, Japan) and a preparative column (Shodex Sugar KS2002, 300 × 20 mm, Showa Denko, Tokyo, Japan) held at 50 °C, with HPLC-grade water (Carl Roth, Karlsruhe, Germany) as the eluent, at a flow rate of 0.75 mL min⁻¹. The WSC were detected by refractive index measurement (Shodex RI-101, Showa Denko, Tokyo, Japan) and concentrations quantified by comparing sample peak areas against reference calibration curves of pure and mixed standards of analytical grade inulin, sucrose, glucose and fructose (all from Merck, Darmstadt, Germany). Knowing when the individual carbohydrates eluted from the preparative column (Fig. 3), fractions of fructan, sucrose, glucose, and fructose were individually collected in test tubes.

¹³C analysis of biomass and water-soluble carbohydrate components

The $\delta^{13}C$ of biomass samples was determined for all shoot and root replicates, as in Lattanzi et al. [27]. The stored samples were thawed, re-dried at 40 °C for 24 h and stored in exsiccator vessels. Aliquots of 0.70 ± 0.05 mg of the shoot and root materials were weighed and packed into tin cups $(3.3\times5$ mm, IVA Analysentechnik, Meerbusch, Germany). These were then combusted in an elemental analyzer (NA 1110, Carlo Erba Instruments, Milan, Italy) interfaced (Conflo III, Finnigan MAT, Bremen, Germany) to a continuous-flow isotope-ratio mass spectrometer (CF-IRMS, Delta Plus, Finnigan MAT, Bremen, Germany) which measured $\delta^{13}C$. A solid internal laboratory standard (SILS, fine ground wheat flour) was measured as a reference after every tenth sample

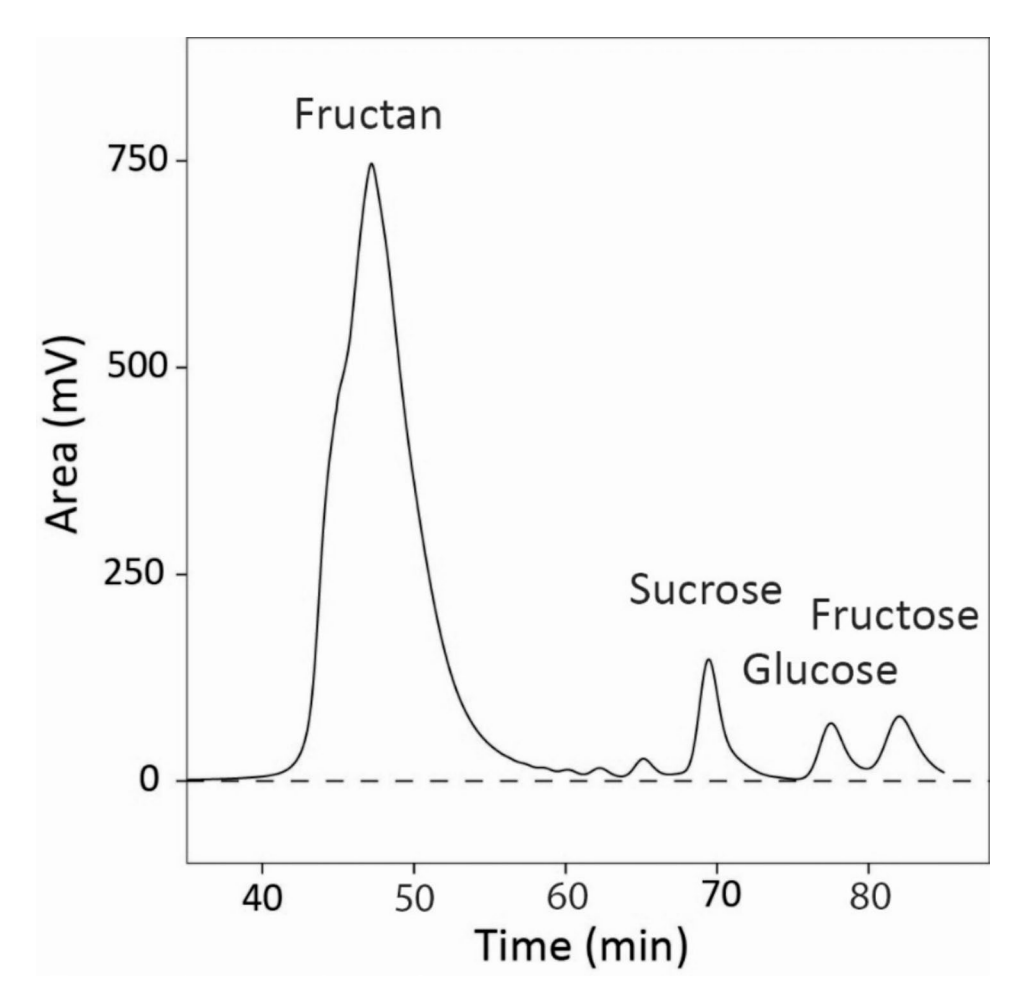


Fig. 3 Typical HLPC elution diagram for water-soluble carbohydrates (WSC) extracted from whole shoot biomass of *Lolium perenne*. The fractions corresponding to fructan, sucrose, glucose and fructose are indicated in the panel. Note the two small peaks on the lefthand side of the sucrose peak, which likely corresponded (from right to left) to fructan tri-saccharides and tetra-saccharides. The thin grey line represents the baseline. The total elution time was about 90 min following sample injection. The sample was taken from plants grown in 800 μ mol mol⁻¹ [CO₂]

Zhu et al. Plant Methods (2025) 21:111 Page 9 of 17

to correct for possible instrument drift. All samples and SILS were measured against a laboratory working standard CO_2 gas, which was previously calibrated against a secondary isotope standard (IAEA-CH6; calibration accuracy $\pm 0.06\%$ SD). The long-term precision given as the SD of repeated measurements of the SILS was < 0.2‰.

Aliquots of approximately 0.70 mg of the different WSC fractions were transferred to tin cups, dried at 60 °C for 24 h, and then analyzed for their δ^{13} C using the same CF-IRMS system as above.

$\delta^{13}C$ of WSC-free biomass

The $\delta^{13}C$ of WSC free biomass ($\delta^{13}C_{WSC-free\ biomass}$) was determined from isotopic mass balance for a given biomass sample X, thus.

$$\begin{array}{l} \delta^{13} {\rm C_{WSC-free\; biomass}} = \\ (\delta^{13} {\rm C_{biomass}} \; W_{\rm biomass} - \\ \delta^{13} {\rm C_{WSC}} \; W_{\rm WSC}) \, / \, (W_{\rm biomass} - W_{\rm WSC}), \end{array} \tag{3}$$

with $W_{\rm biomass}$ and $W_{\rm WSC}$ the C mass in biomass and in total WSC of a give sample, and $\delta^{13}C_{\rm biomass}$ and $\delta^{13}C_{\rm WSC}$ the of $\delta^{13}C$ of the biomass and WSC extracted from that biomass sample. Note that the isotopic mass balance accounts explicitly for isotope fractionation (^{13}C discrimination) effects on bulk shoot biomass and WSC as expressed in their $\delta^{13}C_{\rm biomass}$ and $\delta^{13}C_{\rm WSC}$ (cf. Eq. 1).

δ^{13} C of respired CO₂

The δ^{13} C of respired CO₂ (δ^{13} C_{P_p}) was obtained as [25]:

$$\delta^{13}C_{Rn} = (\delta^{13}C_{inlet} F_{inlet} - \delta^{13}C_{outlet} F_{outlet}) / (F_{inlet} - F_{outlet}),$$
 (4)

with $\delta^{13}C_{\text{inlet}}$ and $\delta^{13}C_{\text{outlet}}$ the (measured) $\delta^{13}C$ of CO_2 entering and leaving the growth chamber, respectively, and F_{inlet} and F_{outlet} the fluxes of CO_2 (µmol s⁻¹) entering and leaving the chamber during the dark period.

Estimation of C contamination

The fraction contamination of the C $(f_{\rm contam})$ contained in any one type X of sample (with X standing for biomass or WSC fraction (fructan, sucrose, glucose or fructose) or respired CO $_2$ was determined as $f_{\rm contam~X}=1-d\delta^{13}C_{\rm X~actual}/d\delta^{13}C_{\rm Ref}$ (Eq. 2) as explained in the Background section. In this, $d\delta^{13}C_{\rm X}$ corresponds to the measurements-based $\delta^{13}C$ -difference between samples of the same type collected simultaneously from parallel chambers, where one was supplied with ^{13}C -depleted CO $_2$ and the other with ^{13}C -enriched CO $_2$. Meanwhile, $d\delta^{13}C_{\rm Ref}$ refers to an estimation of the contamination-free $\delta^{13}C$ -difference between the ^{13}C -depleted and ^{13}C -enriched CO $_2$ supplied to the chambers for the reference sample

(see below and Table 1). For calculation of $\delta^{13}C_{Ref}$ for each chamber, we first estimated the uncontaminated $\delta^{13}C$ of CO_2 at the outlet of the chamber ($\delta^{13}C_{outlet\ pure}$), by solving for $\delta^{13}C_{outlet}$ the Eq. 10 of Evans et al. [34]

$$\begin{array}{l} \delta^{13}C_{outlet\;pure} = \\ (\Delta^{13}C + \xi \, \delta^{13}C_{inlet} \, (\Delta^{13}C/1000) + \\ \xi \delta^{13}C_{inlet}) \, / \, ((\Delta^{13}C/1000)(\xi - 1) + \xi), \end{array} \tag{5}$$

with $\Delta^{13}C$ given in per mil (‰). In Eq. 5, $\delta^{13}C_{\text{inlet}}$ corresponds to the $\delta^{13}C$ of CO_2 as measured at the inlet of the growth chamber. $\Delta^{13}C$ was set to 21‰, a value close to that estimated for shoot biomass of perennial ryegrass or temperate (C_3) grassland in the absence of drought stress in many works [53–56]. ξ was obtained as [34]:

$$\xi = C_{\text{inlet}} / (C_{\text{inlet}} - C_{\text{outlet}}),$$
 (6)

with $C_{\rm inlet}$ and $C_{\rm outlet}$ the ${\rm CO_2}$ concentration in air as measured at the inlet and outlet of the growth chamber, respectively.

Next, we estimated $\delta^{13}C_{ReP}$ the contamination-free $\delta^{13}C$ representative for all functional parameters (biomass fractions, WSC components or dark respiration; see below) as,

$$\delta^{13}C_{Ref} = (\delta^{13}C_{inlet} \times F_{inlet} - (\delta^{13}C_{outlet pure} \times F_{outlet}) / (F_{inlet} - F_{outlet}).$$
(7)

Then, $d\delta^{13}C_{Ref}$ the uncontaminated $\delta^{13}C$ -difference between $\delta^{13}C_{ref}$ estimates for the parallel chambers, was obtained as the numerical difference between the two $\delta^{13}C_{Ref}$ values. In the process, we used $d\delta^{13}C_{Ref}$ in all calculations of $f_{\rm contam}$ for all types of samples and treatments, thus— for the time being— positing that $\Delta^{13}C$ did not differ between treatments and that eventual post-photosynthetic discrimination was constant. In a second step, however, we explored the sensitivity of contamination estimates to variation of $\Delta^{13}C$ during daytime gas exchange measurements, as observed in the different $[CO_{\gamma}]$ treatments.

Statistical analysis

One-way analysis of variance (ANOVA) with Tukey's HSD post hoc tests for pairwise comparisons was conducted to explore the effect of CO_2 treatments on the contamination (f_{contam}) of biomass (n=2–4) and WSC components (n=2–4). For f_{contam} of dark respiration (n=17–39), a linear mixed-effects model (LMM) was fitted using the lme4 package [57]. The model included [CO_2] treatment as a fixed effect and sampling day as a random effect to account for temporal pseudo-replication. The significance of fixed effects was evaluated

Zhu et al. Plant Methods (2025) 21:111 Page 10 of 17

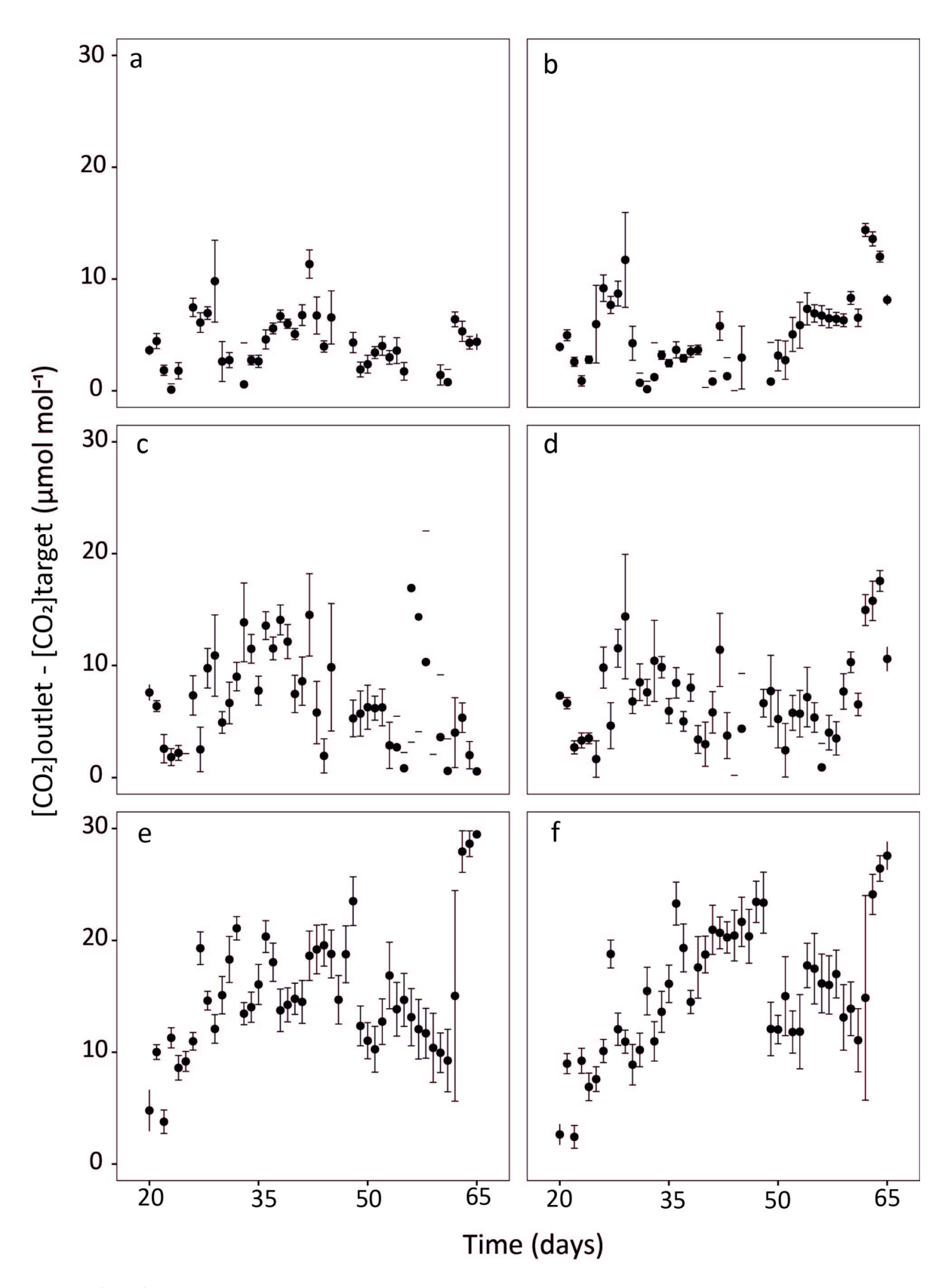


Fig. 4 (See legend on next page.)

Zhu et al. Plant Methods (2025) 21:111 Page 11 of 17

(See figure on previous page.)

Fig. 4 CO₂ concentration difference between chamber outlet ($[CO_2]_{outlet}$) and the set target $[CO_2]$ ($[CO_2]_{target}$) between day 20 and 65 in experimental runs with target $[CO_2]$ of: (**a**, **b**) 200, (c, d) 400 and (e, f) 800 µmol mol⁻¹. Growth chambers were supplied with either ¹³C-depleted CO_2 ($\delta^{13}C_{CO2}$ -43.5%) (panels **a**, **c** and **e**) or ¹³C-enriched CO_2 ($\delta^{13}C_{CO2}$ -5.6%); right) (panels **b**, **d**, **f**). Measurements taken during the first 45 min of the light period, or following the opening of the chamber, or exceeding 1.5 times the interquartile range (outliers) were eliminated from the data set. Data points and error bars represent daily means \pm SD (n = 9–23)

using sequential (Type I) likelihood ratio tests, and post hoc pairwise comparisons performed with Tukey's HSD using the emmeans package [58]. All statistical analyses were performed in R v.4.0.2 [59]. The R-package ggplot2 [60] was used for data visualization.

Results

Variation of $[CO_2]$ and $\delta^{13}C_{CO2}$ during the experiment

The daytime mean CO_2 concentration at the chamber outlet varied little (coefficient of variation < 2%) between 20 and 65 days, and on average was 4.0 (±4.3 SD), 7.2 (±6.2 SD) and 13.9 (±8.3 SD) µmol mol⁻¹ higher than the target [CO_2] of 200, 400 and 800 µmol mol⁻¹, respectively (Fig. 4). These differences corresponded to mean relative deviations from target [CO_2] of ≤2% in every treatment. Importantly, these deviations did not differ (P > 0.05) between chambers receiving ¹³C-depleted and ¹³C-enriched CO_2 (Fig. 4).

Meanwhile, the δ^{13} C of CO_2 at the chamber outlet ($\delta^{13}C_{CO2 \text{ outlet}}$) relative to the chamber inlet ($\delta^{13}C_{CO2 \text{ inlet}}$) increased by several ‰ during daytime until day 30 to 35 (Fig. 5) when canopies became closed. Thereafter, the increase of δ^{13} C at the chamber outlet relative to that at the inlet was relatively stable until the end of the experiments (Fig. 5). Again, these effects were the same in chambers receiving 13 C-depleted and 13 C-enriched CO_2 (Fig. 5).

Contamination

ANOVA provided no evidence for a significant effect of $[CO_2]$ treatments on the fraction of contaminating $C(f_{contam})$ in any parameter of the study, except for respired CO_2 (Table 2).

Biomass components (shoot and root), including WSC-free shoot biomass, and the different WSC fractions shared a very similar contamination of (on average) 3.3% ($\pm 0.9\%$ SD), which was—moreover—close to that of respired CO₂ at both 200 and 400 μ mol mol⁻¹ CO₂ (compare in Table 3), and did not differ significantly (P=0.84) between the latter. Conversely $f_{\rm contam}$ of respired CO₂ was slightly negative at 800 μ mol mol⁻¹ CO₂, but not significantly different from zero, and significantly smaller than at 200 and 400 μ mol mol⁻¹ CO₂ (P<0.05 for both comparisons). Significantly, the uncertainty for the individual estimates of contamination (represented by the SD) was not much smaller than the contamination estimates for most biomass and WSC parameters (average SD 2.3%)

and corresponded to an average coefficient of variation CV = SD/mean of 67%.

 CO_2 treatment effects were tested with one-way ANOVA for biomass and WSC components (n = 2-4) and a linear mixed model for dark respiration (n = 17-39).

 $f_{\rm contam}$ was determined for canopy-scale dark respiration for days 38 to 65, and bulk shoot and root C, and fructan, sucrose, glucose and fructose extracted and purified from shoot biomass sampled at the beginning of the light period on day 65. In all experiments, growth chambers were maintained near target [CO₂] of 200, 400 or 800 μmol mol⁻¹ using one of two CO₂ sources, a relatively ¹³C-depleted (δ¹³C -43.5‰) or ¹³C-enriched source ($\delta^{13}\mathrm{C}$ -5.6%). f_contam for dark respiration was determined during periods of steady-state gas exchange of chambers. That is, measurements in the first 45 min of a dark period or following the opening of the chamber were removed, and values over 1.5 × IQR (Interquartile Range) away from the mean were removed as outliers. Except for $[CO_2]$ and $\delta^{13}C_{CO2}$, all conditions were kept the same in all chambers (see Materials and Methods). The means and standard deviations (SD) are presented for each treatment and were calculated based on daily replicates (n=17-39) for dark respiration measurements or chamber-level replicates (n = 2-4) for all other parameters. Different superscript letters in the same row indicate a significant (P<0.05) effect of [CO₂] treatments.

The effect of varying discrimination on estimates of contamination

As illustrated by the methodology, assumptions of $\Delta^{13}\mathrm{C}$ impact estimations of contamination (i.e. f_{contam}) via the determination of the $d\delta^{13}\mathrm{C}_{\mathrm{Ref}}$ -values (see Eqs. 2, 5 and 7). Significantly, we observed [CO_2] dependent variation of $\Delta^{13}\mathrm{C}$ during daytime net CO_2 exchange ($\Delta^{13}\mathrm{C}_{\mathrm{N}}$) counter to expectations: thus, $\Delta^{13}\mathrm{C}_{\mathrm{N}}$ increased from approx. 19 to 23% between 200 and 800 $\mu\mathrm{mol}$ mol $^{-1}$ of CO_2 (Table S1). Thus, our literature-based assumption of constant $\Delta^{13}\mathrm{C}$ (= 21%) must have biased estimations of f_{contam} to some degree. The numerical effect of this $\Delta^{13}\mathrm{C}$ -dependent variation on estimates of f_{contam} is explored in Fig. 6.

This analysis demonstrated a negative relationship between estimates of $f_{\rm contam}$ and assumed $\Delta^{13}{\rm C}$, with a 0.44% decrease of the estimated $f_{\rm contam}$ for a 6% decrease of $\Delta^{13}{\rm C}$ from 18 to 24%. The maximum error on estimates of $f_{\rm contam}$ which resulted from neglecting the [CO $_2$] treatment effect on $\Delta^{13}{\rm C}$ as observed here was 0.3%, but did not change conclusions with respect to the

Zhu et al. Plant Methods (2025) 21:111 Page 12 of 17

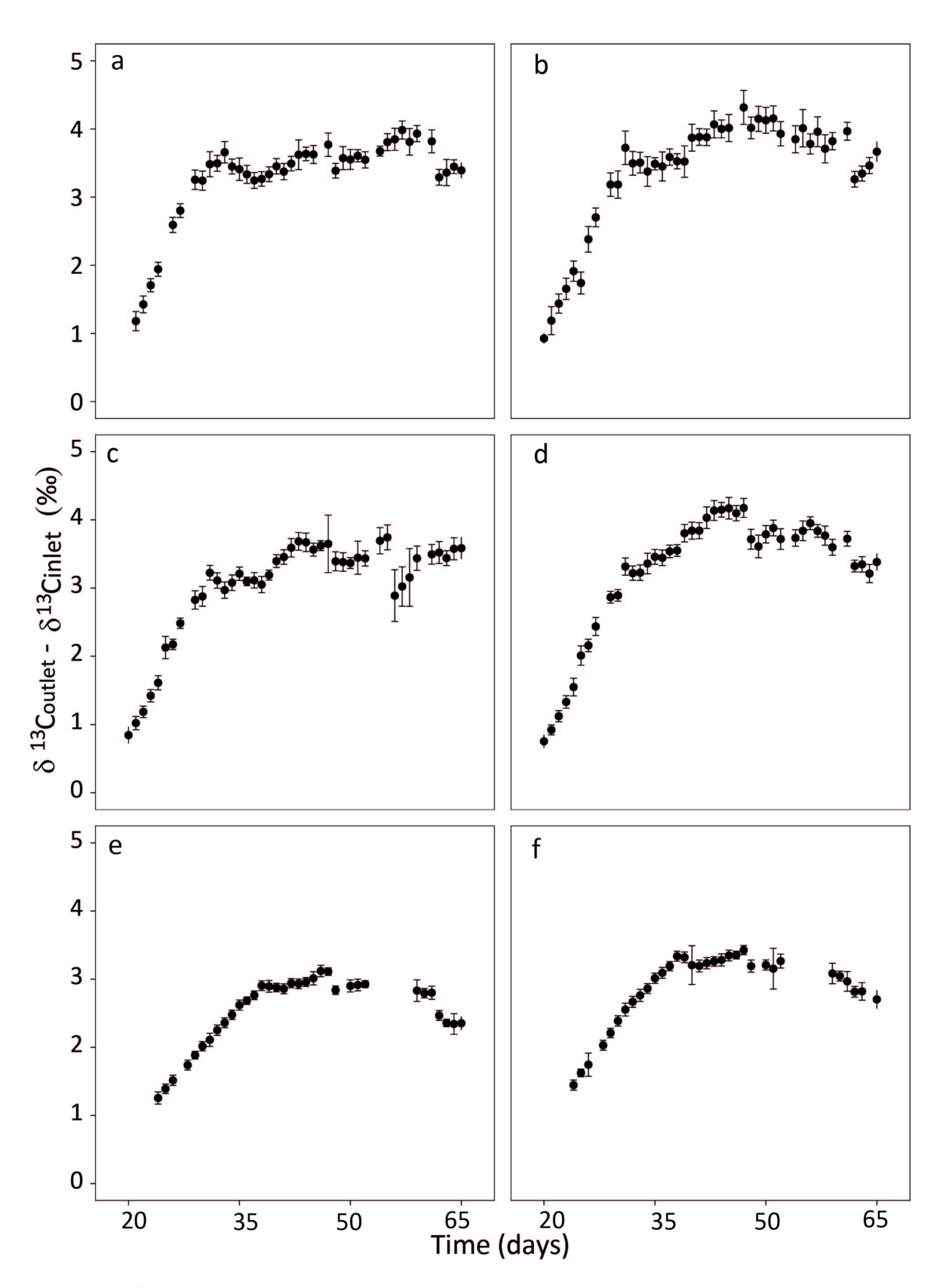


Fig. 5 (See legend on next page.)

Zhu et al. Plant Methods (2025) 21:111 Page 13 of 17

(See figure on previous page.)

Fig. 5 The δ^{13} C-difference between CO₂ measured at the chamber outlet (δ^{13} C_{CO2 outlet}) and inlet (δ^{13} C_{CO2 outlet}) over time (δ^{13} C_{CO2 outlet} - $\delta^$

non-significance (or significance) of the $[CO_2]$ treatment effect on f_{contam} (Table S2).

Discussion

Contamination was small and similar for all parameters

To the best of our knowledge, this work presents the first systematic, comprehensive and quantitative assessment of isotopic contamination artifacts in a labelling experiment. This analysis determined a very small contamination of samples, which was- moreover- closely similar for a range of functional parameters (biomass fractions, WSC components and respired CO₂) and not significantly different for the different [CO₂] treatments (Tables 2 and 3), except for respiration at high CO₂ which was insignificant. Lack of statistical significance for the [CO₂] effect on contamination was not intuitive based on the expectation that incursion of a defined volume of extraneous CO2 into labelling vessels would cause a (proportionally) greater mixing with a low than a high set CO2 concentration, under ceteris paribus conditions. Indeed, there was a non-significant tendency for a lower contamination at 800 µmol mol-1 [CO2] than at 200 and 400 μ mol mol⁻¹, especially for the biomass components. Also, there was a significant (negative) [CO₂] treatmenteffect on f_{contam} for respired CO₂, which accorded with the expected (relatively) smaller extraneous CO2 incursion at 800 μ mol mol⁻¹ [CO₂]. Yet, these effects were very small, and not even considering the [CO₂] treatmenteffect on Δ^{13} C (Table S1) did change conclusions with respect to the (non-)significance of [CO₂] treatmenteffect on $f_{\rm contam}$ (Table S2). The fact that contamination was generally very small certainly contributed to the absence of statistical significance via a small signal to error ratio (which is- basically- the inverse of the CV) in the data. In that, the experimental error was not large at all (see also Materials and Methods). This may be recognized by translating a given contamination-% into the δ¹³C-difference (between ¹³C-enriched and ¹³C-depleted chambers), which is required to return a certain contamination-%. For instance, a 3% contamination corresponded to an approx. 1.1% smaller δ^{13} C-difference between the measurements $(d\delta^{13}C_X)$ than the predicted uncontaminated reference estimates $(d\delta^{13}C_{Ref})$. By comparison, with a very good average, whole-system SD of (say) 0.4‰ for the $\delta^{13}C_x$ data – which integrates all errors from CO_2 administration over an extended period of time, labelling chamber operation (including adjustments in flow rates, changes of CO_2 flasks, variation of $\delta^{13}C_{CO_2}$ in the chambers, and sample collection and preparation)— error propagation yields a (whole system) SD of 0.57‰ on average for the $d\delta^{13}C_X$ data. Given the average 1.1‰-signal associated with a 3% contamination (see above), this SD of 0.57‰ translates to a CV of 52% for the contamination estimate which is not far from that observed here for the biomass and WSC components (average 67%).

Clearly, increasing the isotopic spread between the two CO_2 sources used in experiments would help to increase the signal-to-error ratio of contamination estimation. In our laboratory we have used commercial sources of CO_2 with $\delta^{13}C$ as high as -2% and as low as -50%, which yields an isotopic spread which is somewhat larger than that found here (48% vs. 38%). Of course, using artificially ^{13}C -enriched CO_2 sources [31] could further reduce the relative experimental error, including that of contamination estimations, and therefore increase to some degree the sensitivity of $^{13}CO_2/^{12}CO_2$ tracer studies, albeit at much greater financial cost for the labelling CO_2 .

Importantly, in the present work contamination of the different WSC components was very similar to whole shoot biomass (from which they were extracted) and WSC-free shoot biomass. Based on this close similarity, we find no indication for any additional contamination which might have occurred during WSC extraction, separation and analysis. Given absence of evidence for additional contamination of WSC, it is futile to discuss any such eventual sources, except for acknowledging the effectiveness of the protocols and the cleanliness of the laboratory work.

Strikingly, contamination of respiratory CO₂ at 200 and 400 μmol mol⁻¹ CO₂ was also close to that of biomass and- specifically- WSC components. This observation agrees with the expectation that in vivo contamination of the respiratory substrate (specifically WSC) was the dominant factor explaining contamination of respired CO₂ at least in these treatments. It is well accepted that nonstructural carbohydrates are the dominant source of substrate for dark respiration [32, 61]. At the same time, this would also suggest that no additional contamination with extraneous CO2 occurred during respiration measurements. This is also unsurprising given the fact that dark respiration measurements occurred during (undisturbed) isotopic steady-state for gas exchange during periods when chambers had not been opened for at least 45 min previously. Meanwhile, we cannot explain the observation that respired CO₂ was apparently uncontaminated at Zhu et al. Plant Methods (2025) 21:111 Page 14 of 17

Table 2 Significance (*P*-value) of [CO₂] treatment effects on contamination (*f*_{contam}) parameters

	CO ₂ effect significance
	(P-value)
Biomass components	
Shoot	0.787
Root	0.219
Water-soluble carbohydrates	
Fructan	0.374
Sucrose	0.972
Glucose	0.816
Fructose	0.759
WSC-free shoot biomass	0.358
Dark respiration	< 0.001

Table 3 The fraction of contaminating $C(f_{contam}, \%)$ in diverse sample types

Parameter	CO ₂ concentration (µmol mol ⁻¹)		
	200	400	800
	f _{contam} , %		
Biomass components			
Shoot	3.9 (0.2)	4.1 (2.3)	2.7 (2.8)
Root	4.0 (0.7)	4.6 (1.6)	2.0 (1.4)
Water-soluble carbohydrates			
Fructan	3.7 (0.7)	2.2 (1.8)	4.8 (2.9)
Sucrose	3.4 (4.4)	2.7 (3.0)	3.4 (5.1)
Glucose	3.1 (4.2)	4.8 (2.3)	3.3 (5.1)
Fructose	3.7 (3.3)	4.5 (1.4)	1.9 (7.6)
WSC-free shoot biomass	3.6 (0.3)	4.3 (1.8)	2.1 (1.1)
Dark respiration	3.5 (2.7) ^a	3.5 (4.5) ^a	-2.4 (5.2) ^b

800 μ mol mol⁻¹ CO₂, albeit this estimate was associated with relatively large uncertainty. Particularly, we have not found any chamber effects on any morpho-physiological parameters studied in the work of Baca Cabrera et al. [48–50], which occurred just prior to the tests which are presented here.

One question not directly explored by the present analysis is whether the $\delta^{13}C_{CO2}$ of the contaminating source was more similar to the ¹³C-enriched or the ¹³C-depleted CO₂ source used in this work. This question is also of interest for the accuracy of the $\Delta^{13}C_x$ data which can be obtained from the present data. We opine that the actual $\delta^{13}C_{CO2}$ of the extraneous (contaminating) CO_2 was likely close to that of all CO₂ exiting the chambers. Given that the fossil-organic and mineral CO₂ sources were always used in parallel in equal proportions (see Materials and Methods) and CO₂ was ¹³C-enriched by approx. 3‰ inside the chambers (see Fig. 5) due to photosynthetic ^{13}C discrimination, we estimate the $\delta^{13}\text{C}_{\text{CO2}}$ of this fiftyfifty mixture thus $\approx (0.5 \times -43.5\% + 0.5 \times -5.6\%) + 3\%$ = 27.6% (with -43.5% and -5.6%, representing the $\delta^{13}C_{CO2}$ of the fossil-organic and mineral CO₂ supplied to the chambers). This δ^{13} C-value of the total CO₂ leaving the chambers is also close to the δ^{13} C of human-exhaled $\rm CO_2$ (e.g. the experimenters) when this is based on a typical Central European, mainly $\rm C_3$ -based diet [62]. Mixing of the $\rm CO_2$ inside the room housing the labelling facility (in the basement of 'Alte Akademie 12' in Freising-Weihenstephan) with free atmospheric $\rm CO_2$ ($\delta^{13}\rm C_{CO2}$ approx. – 9‰) was likely a very minor factor, as the volume of air in this room was continuously flushed with air from the growth chambers at a high rate. In consequence, we also argue that reasonable $\Delta^{13}\rm C_X$ -values can be obtained by simply averaging the $\Delta^{13}\rm C_X$ -values from the $^{13}\rm C$ -enriched and $^{13}\rm C$ -depleted chambers.

Although not comparable in terms of experimental purpose, system design and level of ¹³C enrichment, the degree of isotopic contamination observed in the present work seems comparable to that of commercial systems which are used to manufacture highly isotopically enriched compounds. Thus, for instance, closed systems [63] specially designed to produce highly isotopically enriched plant compounds with pure ¹³CO₂ gas, achieved a degree of labelling of 96-98 atom-%. Given that isotopic fractionation is suppressed in a closed system [64] with continuous and complete photosynthetic fixation of the supplied substrate CO₂, and also cannot occur for C when the added substrate CO2 contains only one C isotope (pure ¹³C in this case), it would seem that isotopic contamination (with ¹²C) in [63] was probably very similar at approx. 2–4%.

In the present work, contamination was likely dominated by extraneous CO_2 entering the growth chambers during light periods when these had to be accessed for experimental or maintenance purposes (e.g. changes of defective light sources). Unfortunately, we did not sample the 12 days-old seedlings when we started the $\delta^{13}\mathrm{C}_{\mathrm{CO}2}$ treatments, so we cannot quantify the possible contribution of the experimental starting material (see Background) to the integral contamination estimate. However, if we make assumptions extrapolated from our first chamber-scale gas exchange measurements, we estimate an experimental starting material-associated contamination of not more than ~1% (compare also plant sizes in Figure S4).

How to deal with contamination in tracer data evaluation?

Of course, the best way to avoid complications with contamination is to avoid contamination altogether. As we emphasize, using air locks in chamber doors and minimizing experimental and maintenance operations inside the chambers during daytime are important contamination avoidance principles in addition to precautions already mentioned in the Discussion sections above. Concerning air locks, there may be a trade-off between their effectiveness in reducing CO_2 incursion when doors are open and the ease of access to the chamber interior that they permit (compare Figures S3A and B). While we

Zhu et al. Plant Methods (2025) 21:111 Page 15 of 17

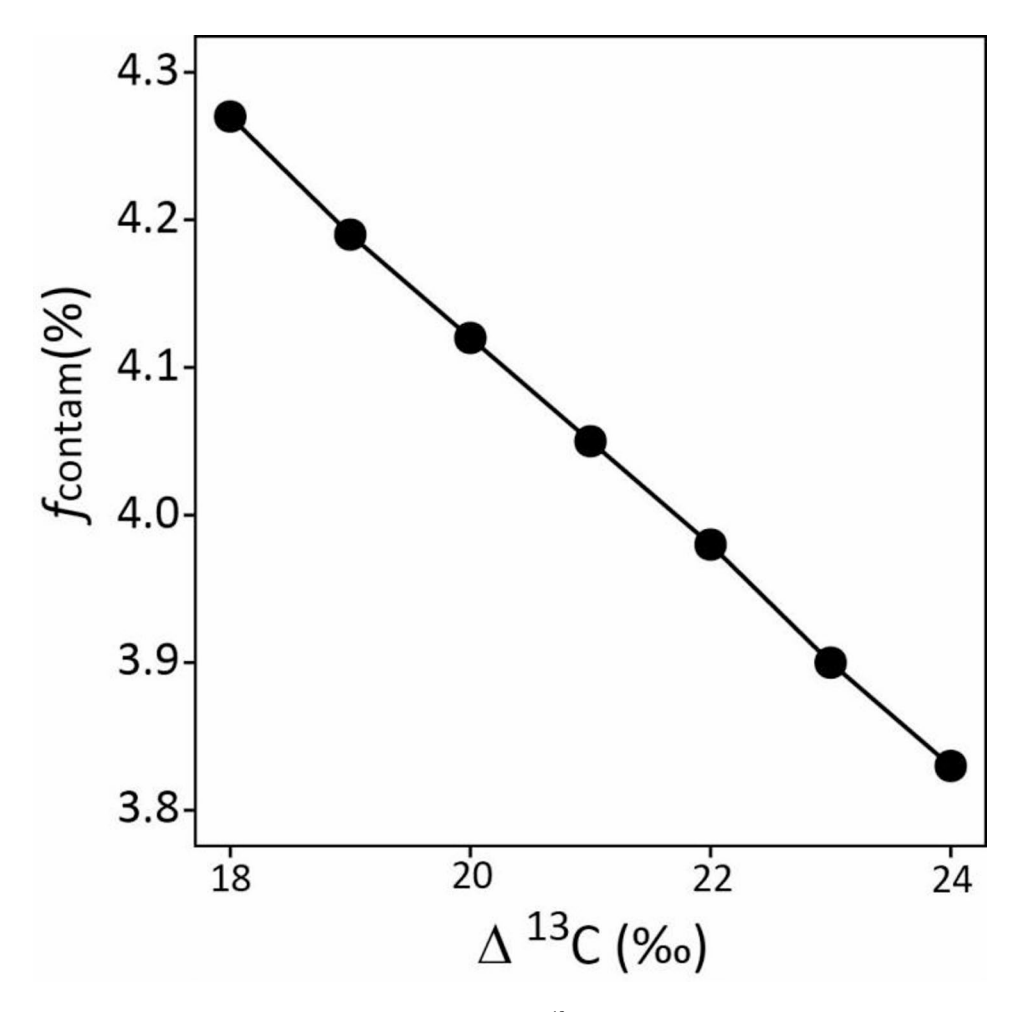


Fig. 6 Sensitivity of contamination-% ($f_{\text{contam'}}$ %) estimates to assumptions of Δ^{13} C in the range of 18 to 24%. The analysis was based on an arbitrary sample with an estimated f_{contam} of 4.05% at Δ^{13} C = 21% (see Materials and Methods)

failed to compare the effectiveness of these two versions of air locks directly, the measurements by Lehmeier et al. [32] do suggest that their airlocks provide excellent proof for their effectiveness (Figure S3B).

The fact that we observed only small contamination, despite of the fact that the study was performed with a highly experimentally-perturbed system, supports our assessment that previous works which were performed with less experimentally disturbed studies in a very similar system [25, 32] should have suffered even less from contamination. This view is supported by the absence of a CO₂ source (¹³C enriched vs. ¹³C-depleted CO₂) effect on measurements of Δ^{13} C during net CO₂ exchange in light [25]. Nevertheless, for instance, Lehmeier et al. [32] did allow for some contamination in their evaluation of the tracer kinetics of respired CO2 when using a very similar, two-chamber system with two distinct $\delta^{13}C_{CO2}$. In that, they used measurements from plants which had grown continuously in the presence of ¹³C-enriched or $^{13}\text{C-depleted}$ CO_2 as the endmembers $(\delta^{13}\text{C}_{\text{new}}$ and $\delta^{13}C_{\text{old}})$ of the isotopic mixing model which they applied to the tracer data. This procedure did correct for an eventual contamination, although it used the assumption that contamination was a constant.

Conclusions

The aim of this work was to quantify systematically and comprehensively C isotopic contamination artefacts which occurred in a > 9 weeks-long experiment with continuous exposure of L. perenne plants to one of two C-isotopically distinct natural CO₂ sources, one a ¹³C-depleted fossil-organic source and the other a (relatively) ¹³C enriched mineral source, at one of three [CO₂]-levels: 200, 400 or 800 μmol mol⁻¹ CO₂ in plant growth chambers. The experiments provided an elevated opportunity for contamination due to extensive experimental activities in all chambers during the last two weeks just prior to determination of contamination. Nevertheless, the findings indicated only a low level of contamination (3.3% on average) for biomass and WSC fractions, with no significant effect of [CO₂] on contamination. Thus, our work supports the use of the present ¹³CO₂/¹²CO₂ system and Zhu et al. Plant Methods (2025) 21:111 Page 16 of 17

protocols for quantitative C tracer experiments of plant metabolism across contrasts of $[CO_2]$. Certainly, contamination avoidance principles used (and discussed) here should be adopted also in simpler tracer systems (e.g. one-chamber systems with or without inclusion of CF-IRMS or other online gas isotope analysers) in controlled or field environments [21, 31], especially if such experimental systems do not permit quantification of contamination artifacts, as is usually the case.

Supplementary Information

The online version contains supplementary material available at https://doi.org/10.1186/s13007-025-01431-3.

Supplementary Material 1

Acknowledgements

The project was funded by the Deutsche Forschungsgemeinschaft (DFG SCHN 557/9-1). JZ was supported by the China Scholarship Council (CSC). Anja Schmidt, Monika Michler, Angela Ernst-Schwärzli, Laura Dorn, Wolfgang Feneis and Richard Wenzel are thanked for expert assistance with maintenance of the gas exchange facility (WF, RW), sample collection and processing (AS, MM, AES) and carbohydrate analyses (AS, LD).

Author contributions

HS and RTH acquired funding of the project. JZ, RS and HS conceived the idea of the study. JZ, RS, JCBC and RTH performed the work. JZ, HS and RS wrote the paper. JZ, RTH, JCBC, RS and HS revised the paper.

Funding

Open Access funding enabled and organized by Projekt DEAL. Deutsche Forschungsgemeinschaft (DFG SCHN 557/9-1).

Data availability

The data supporting the findings of this study are available from the corresponding authors upon reasonable request.

Declarations

Ethics approval and consent to participate

Not applicable (the study involved no animals and no human participants, human data or human tissue).

Consent for publication

Not applicable.

Competing interests

The authors declare no competing interests.

Author details

¹Technische Universität München, Lehrstuhl für Grünlandlehre, Alte Akademie 12, 85354 Freising-Weihenstephan, Germany

²State Key Laboratory of Microbial Technology, Shandong University, Qingdao, Shandong, China

³Institute of Bio- and Geoscience, Forschungszentrum Jülich GmbH, Agrosphere (IBG-3), Jülich, Germany

⁴Crop Physiology, Technische Universität München, 85354 Freising-Weihenstephan, Germany

Received: 27 May 2025 / Accepted: 3 August 2025 Published online: 11 August 2025

References

- Allen DK, Libourel IGL, Shachar-Hill Y. Metabolic flux analysis in plants: coping with complexity. Plant Cell Environ. 2009;32:1241–57.
- 2. Allen DK, Young JD. Tracing metabolic flux through time and space with isotope labeling experiments. Curr Opin Biotechnol. 2020;64:100–8.
- Bassham JA, Benson AA, Kay LD, Harris AZ, Wilson AT, Calvin M. The path of carbon in photosynthesis. XXI. The Cyclic regeneration of carbon dioxide acceptor. J Am Chem Soc. 1954;76:1760–70.
- Brüggemann N, Gessler A, Kayler Z, Keel SG, Badeck F, Barthel M, et al. Carbon allocation and carbon isotope fluxes in the plant-soil-atmosphere continuum: a review. Biogeosciences. 2011;8:3457–89.
- De Visser R, Vianden H, Schnyder H. Kinetics and relative significance of remobilized and current C and N incorporation in leaf and root growth zones of Iolium Perenne after defoliation: assessment by ¹³C and ¹⁵N steady-state labelling. Plant Cell Environ. 1997;20:37–46.
- Epron D, Bahn M, Derrien D, Lattanzi FA, Pumpanen J, Gessler A, et al. Pulselabelling trees to study carbon allocation dynamics: a review of methods, current knowledge and future prospects. Tree Physiol. 2012;32:776–98.
- 7. Schnyder H, Ostler U, Lehmeier C, Wild M, Morvan-Bertrand A, Schäufele R, et al. Tracing carbon fluxes: resolving complexity using isotopes. In: Matyssek R, Schnyder H, Oßwald W, Ernst D, Munch JC, Pretzsch H, editors. Growth and defence in plants. Berlin: Springer 2012;157–73.
- Schnyder H, Ostler U, Lehmeier CA. Respiratory turn-over and metabolic compartments: from the design of tracer experiments to the characterization of respiratory substrate-supply systems. In: Tcherkez G, Ghashghaie J, editors. Plant respiration: metabolic fluxes and carbon balance. Cham: Springer; 2017;161–79.
- Schwender J, Ohlrogge J, Shachar-Hill Y. Understanding flux in plant metabolic networks. Curr Opin Plant Biol. 2004;7:309–17.
- Kölling K, Müller A, Flütsch P, Zeeman SC. A device for single leaf labelling with CO₂ isotopes to study carbon allocation and partitioning in Arabidopsis Thaliana. Plant Methods. 2013;9:45.
- Kuzyakov Y, Gavrichkova O. Time lag between photosynthesis and carbon dioxide efflux from soil: a review of mechanisms and controls. Glob Chang Biol. 2010;16:3386–406.
- Lattanzi FA, Berone GD, Feneis W, Schnyder H. ¹³C-labelling shows the effect of hierarchy on the carbon gain of individuals and functional groups in dense field stands. Ecology. 2012;93:169–79.
- 13. Roscher A, Kruger NJ, Ratcliffe RG. Strategies for metabolic flux analysis in plants using isotope labelling. J Biotechnol. 2000;77:81–102.
- Sharkey TD. Discovery of the canonical Calvin-Benson cycle. Photosynth Res. 2019;140:235–52.
- Bergman ME, Gonzáles-Cabanelas D, Wright LP, Walker BJ, Phillips MA. Isotope ratio-based quantification of carbon assimilation highlights the role of plastidial isoprenoid precursor availability in photosynthesis. Plant Methods. 2021;17:32. https://doi.org/10.1186/s13007-021-00732-7
- Treves H, Kuken A, Arrivault S, Ishihara H, Hoppe I, Erban A, et al. Carbon flux through photosynthesis and central carbon metabolism show distinct patterns between algae, C₃ and C₄ plants. Nat Plants. 2022;8:78–91.
- Gebbing T, Schnyder H, Kühbauch W. The utilization of pre-anthesis reserves in grain filling of wheat. Assessment by steady-state ¹³CO₂/¹²CO₂ labelling. Plant Cell Environ. 1999:22:851–8.
- Ratcliffe RG, Shachar-Hill Y. Measuring multiple fluxes through plant metabolic networks. Plant J. 2006;45:490–511.
- Deléens E, Gregory N, Bourdu R. Transition between seed reserve use and photosynthetic supply during development of maize seedlings. Plant Sci Lett. 1984;37:35–9.
- Meharg AA. A critical review of labeling techniques used to quantify rhizosphere carbon-flow. Plant Soil. 1994;166:55–62.
- Gamnitzer U, Schäufele R, Schnyder H. Observing ¹³C labelling kinetics in CO₂ respired by a temperate grassland ecosystem. New Phytol. 2009;184:376–86.
- Schnyder H. The role of carbohydrate storage and redistribution in the source-sink relations of wheat and barley during grain filling

 – a review. New Phytol. 1993;123:233

 –45.
- Deléens E, Pavlidès D, Queiroz O. Application du traçage isotopique naturel par Le ¹³C à La mesure du renouvellement de La Matière foliaire Chez Les Plantes En C₃. Physiol Vég. 1983;21:723–9.
- Schnyder H. Long-term steady-state labelling of wheat plants by use of natural ¹³CO₂/¹²CO₂ mixtures in an open, rapidly turned-over system. Planta. 1992:187:128–35.
- 25. Schnyder H, Schäufele R, Lötscher M, Gebbing T. Disentangling CO_2 fluxes: direct measurements of mesocosm-scale natural abundance $^{13}CO_2/^{12}CO_2$

Zhu et al. Plant Methods (2025) 21:111 Page 17 of 17

- gas exchange, 13 C discrimination, and labelling of CO $_2$ exchange flux components in controlled environments. Plant Cell Environ. 2003;26:1863–74. Gong XY, Schäufele R, Feneis W, Schnyder H. 13 CO $_2$ / 12 CO $_2$ exchange fluxes in
- Gong XY, Schäufele R, Feneis W, Schnyder H. ¹³CO₂/¹²CO₂ exchange fluxes in a clamp-on leaf cuvette: disentangling artefacts and flux components. Plant Cell Environ. 2015;38:2417–32.
- Lattanzi FA, Schnyder H, Thornton B. The sources of carbon and nitrogen supplying leaf growth. Assessment of the role of stores with compartmental models. Plant Physiol. 2005;137:383–95.
- Lehmeier CA, Schäufele R, Schnyder H. Allocation of reserve-derived and concurrently assimilated carbon and nitrogen in seedlings of Helianthus annuus under subambient and elevated CO₂ growth conditions. New Phytol. 2005;168:613–21.
- Klumpp K, Schäufele R, Lötscher M, Lattanzi FA, Feneis W, Schnyder H. C-isotope composition of CO₂ respired by shoots and roots: fractionation during dark respiration? Plant Cell Environ. 2005;28:241–50.
- Lötscher M, Klumpp K, Schnyder H. Growth and maintenance respiration for individual plants in hierarchically structured canopies of medicago sativa and Helianthus annuus: the contribution of current and old assimilates. New Phytol. 2004;164:305–16.
- Lattanzi FA, Ostler U, Wild M, Morvan-Bertrand A, Decau M-L, Lehmeier CA, et al. Fluxes in central carbohydrate metabolism of source leaves in a fructanstoring C₃ grass: rapid turnover and futile cycling of sucrose in continuous light under contrasted nitrogen nutrition status. J Exp Bot. 2012;63:2363–75.
- Lehmeier CA, Lattanzi FA, Schäufele R, Wild M, Schnyder H. Root and shoot respiration of perennial ryegrass are supplied by the same substrate pools: assessment by dynamic ¹³C labelling and compartmental analysis of tracer kinetics. Plant Physiol. 2008;148:1148–58.
- Ostler U, Schleip I, Lattanzi FA, Schnyder H. Carbon dynamics in aboveground biomass of co-dominant plant species in a temperate grassland ecosystem: same or different? New Phytol. 2016;210:471–84.
- Evans JR, Sharkey TD, Berry JA, Farquhar GD. Carbon isotope discrimination measured concurrently with gas exchange to investigate CO₂ diffusion in leaves of higher plants. Funct Plant Biol. 1986;13:281–92.
- 35. Farquhar GD, O'Leary MH, Berry JA. On the relationship between carbon isotope discrimination and the intercellular carbon dioxide concentration in leaves. Funct Plant Biol. 1982;9:121–37.
- Farquhar GD, Ehleringer JR, Hubick KT. Carbon isotope discrimination and photosynthesis. Annu Rev Plant Physiol Plant Mol Biol. 1989;40:503–37.
- Gleixner G, Danier H-J, Werner RA, Schmidt H-L. Correlations between the ¹³C content of primary and secondary plant products in different cell compartments and that in decomposing basidiomycetes. Plant Physiol. 1993;102:1287–90.
- Badeck FW, Tcherkez G, Nogués S, Piel C, Ghashghaie J. Post-photosynthetic fractionation of stable carbon isotopes between plant organs - a widespread phenomenon. Rapid Commun Mass Spectrom. 2005;19:1381–91.
- 39. Bowling DR, Pataki DE, Randerson JT. Carbon isotopes in terrestrial ecosystem pools and CO₂ fluxes. New Phytol. 2008;178:24–40.
- Cernusak LA, Tcherkez G, Keitel C, Cornwell WK, Santiago LS, Knohl A, et al. Why are non-photosynthetic tissues generally ¹³C enriched compared with leaves in C₃ plants? Review and synthesis of current hypotheses. Funct Plant Biol. 2009;36:199–213.
- Diefendorf AF, Mueller KE, Wing SL, Koch PL, Freeman KH. Global patterns in leaf ¹³C discrimination and implications for studies of past and future climate. Proc Natl Acad Sci USA. 2010;107:5738–43.
- 42. Baca Cabrera JC, Hirl RT, Schäufele R, Zhu J, Liu H, Ogée J et al. 18 O enrichment of leaf cellulose correlated with 18 O enrichment of leaf sucrose but not bulk leaf water in a C_3 grass across contrasts of atmospheric CO_2 concentration and air humidity. https://doi.org/10.21203/rs.3.rs-596094/v1
- 43. Graven H, Keeling RF, Rogelj J. Changes to carbon isotopes in atmospheric ${\rm CO_2}$ over the industrial era and into the future. Glob Biogeochem Cycles. 2020;34:e2019GB006170.
- 44. Epstein S, Zeiri L. Oxygen and carbon isotopic compositions of gases respired by humans. Proc Natl Acad Sci USA. 1988;85:1727–31.
- Yanes Y, Yapp CJ. Indoor and outdoor urban atmospheric CO₂: stable carbon isotope constraints on mixing and mass balance. Appl Geochem. 2010;25:1339–49.
- 46. González J, Remaud G, Jamin E, Naulet N, Martin GG. Specific natural isotope profile studied by isotope ratio mass spectrometry (SNIP–IRMS):

- ¹³C/¹²C ratios of fructose, glucose, and sucrose for improved detection of sugar addition to pineapple juices and concentrates. J Agric Food Chem. 1999;47:2316–21.
- 47. Isaac-Renton M, Schneider L, Treydte K. Contamination risk of stable isotope samples during milling. Rapid Commun Mass Spectrom. 2016;30:1513–22.
- Baca Cabrera JC, Hirl RT, Zhu JJ, Schäufele R, Schnyder H. Atmospheric CO₂ and VPD alter the diel Oscillation of leaf elongation in perennial ryegrass: compensation of hydraulic limitation by stored-growth. New Phytol. 2020;227:1776–89.
- Baca Cabrera JC, Hirl RT, Zhu J, Schäufele R, Ogée J, Schnyder H. ¹⁸O enrichment of sucrose and photosynthetic and nonphotosynthetic leaf water in a C₃ grass– atmospheric drivers and physiological relations. Plant Cell Environ. 2023;46:2628–48.
- Baca Cabrera JC, Hirl RT, Zhu J, Schäufele R, Ogée J, Schnyder H. Half of the ¹⁸O enrichment of leaf sucrose is conserved in leaf cellulose of C₃ grass across atmospheric humidity and CO₃ levels. Plant Cell Environ. 2024;47:2274–87.
- Busch FA, Ainsworth EA, Amtmann A, Cavanagh AP, Driever SM, Ferguson JN, et al. A guide to photosynthetic gas exchange measurements: fundamental principles, best practice and potential pitfalls. Plant Cell Environ. 2024;47:3344–64.
- Gebbing T, Schnyder H. ¹³C labelling kinetics of sucrose in glumes indicates significant refixation of respiratory CO₂ in the wheat ear. Funct Plant Biol. 2001;28:1047–53.
- Schnyder H, Schwertl M, Auerswald K, Schäufele R. Hair of grazing cattle provides an integrated measure of the effects of site conditions and interannual weather variability on δ¹³C of temperate humid grassland. Glob Change Biol. 2006;12:1315–29.
- 54. Köhler IH, Poulton PR, Auerswald K, Schnyder H. Intrinsic water-use efficiency of temperate seminatural grassland has increased since 1857: an analysis of carbon isotope discrimination of herbage from the park grass experiment. Glob Chang Biol. 2010;16:1531–41.
- 55. Köhler IH, Macdonald A, Schnyder H. Nutrient supply enhanced the increase in intrinsic water-use efficiency of a temperate seminatural grassland in the last century. Glob Chang Biol. 2012;18:3367–76.
- Barbosa ICR, Köhler IH, Auerswald K, Lüps P, Schnyder H. Last-century changes of alpine grassland water use efficiency: a reconstruction through carbon isotope analysis of a time-series of Capra Ibex Horns. Glob Change Biol. 2010;16:1171–80.
- Bates D, Mächler M, Bolker B, Walker S, Christensen RH, Singmann H et al. Ime4: linear mixed-effects models using Eigen and S4. R package version1.1–10. https://cran.r-project.org/web/packages/lme4/index.html. Accessed 2 May 2025.
- Lenth RV. emmeans: estimated marginal means, aka least-squares means. R package version 1.8.7. https://CRAN.R-project.org/package=emmeans.Access ed 10 Jun 2022.
- R Core Team. R: A language and environment for statistical computing. Vienna, Austria 2020. https://www.r-project.org/.Accessed 8 Jun 2020.
- Wickham H. ggplot2: elegant graphics for data analysis. New York: Springer 2016.
- Dusenge ME, Duarte AG, Way DA. Plant carbon metabolism and climate change: elevated CO₂ and temperature impacts on photosynthesis, photorespiration and respiration. New Phytol. 2019;221:32–49.
- McCue MD, Passement CA, Rodriguez M. The magnitude of the naturally occurring isotopic enrichment of 13 C in exhaled CO2 is directly proportional to exercise intensity in humans. Comp Biochem Physiol Mol Integr Physiol. 2015;179:164–71.
- Ceranic A, Doppler M, Büschl C, Parich A, Xu K, Koutnik A, et al. Preparation of uniformly labelled 13 C- and 15 N-plants using customized growth chambers. Plant Methods. 2020;16:47. https://doi.org/10.1186/s13007-020-00589-2
- 64. Fry B. Stable isotope ecology. New York, NY, USA: Springer. 2006.

Publisher's note

Springer Nature remains neutral with regard to jurisdictional claims in published maps and institutional affiliations.